Environment International 175 (2023) 107941

Contents lists available at ScienceDirect

Environment International

journal homepage: www.elsevier.com/locate/envint

Full length article

An investigation of PM2.5 concentration changes in Mid-Eastern China before and after COVID-19 outbreak

Yongjun Zhang, Wenpin Wu, Yiliang Li, Yansheng Li *

School of Remote Sensing and Information Engineering, Wuhan University, Wuhan 430079, China

ARTICLE INFO

Handling Editor: Xavier Querol

Keywords:
$PM_{2.5}$ pollution
China's COVID-19 lockdown
Deep learning
Satellite remote sensing

ABSTRACT

With the Chinese government revising ambient air quality standards and strengthening the monitoring and management of pollutants such as $PM_{2.5}$, the concentrations of air pollutants in China have gradually decreased in recent years. Meanwhile, the strong control measures taken by the Chinese government in the face of COVID-19 in 2020 have an extremely profound impact on the reduction of pollutants in China. Therefore, investigations of pollutant concentration changes in China before and after COVID-19 outbreak are very necessary and concerning, but the number of monitoring stations is very limited, making it difficult to conduct a high spatial density investigation. In this study, we construct a modern deep learning model based on multi-source data, which includes remotely sensed AOD data products, other reanalysis element data, and ground monitoring station data. Combining satellite remote sensing techniques, we finally realize a high spital density $PM_{2.5}$ concentration change investigation method, and analyze the seasonal and annual, the spatial and temporal characteristics of $PM_{2.5}$ concentrations in Mid-Eastern China from 2016 to 2021 and the impact of epidemic closure and control measures on regional and provincial $PM_{2.5}$ concentrations. We find that $PM_{2.5}$ concentrations in Mid-Eastern China during these years is mainly characterized by "north-south superiority and central inferiority", seasonal differences are evident, with the highest in winter, the second highest in autumn and the lowest in summer, and a gradual decrease in overall concentration during the year. According to our experimental results, the annual average $PM_{2.5}$ concentration decreases by 3.07 % in 2020, and decreases by 24.53 % during the shutdown period, which is probably caused by China's epidemic control measures. At the same time, some provinces with a large share of secondary industry see $PM_{2.5}$ concentrations drop by more than 30 %. By 2021, $PM_{2.5}$ concentrations rebound slightly, rising by 10 % in most provinces.

1. Introduction

After entering the 21st century, Mid-Eastern China (Beijing Tianjin-Hebei region and East China) has become the main region contributing to China's gross domestic product (GDP) (Xue et al., 2020). At the same time, increasing industrialization and urbanization have led to a rapid increase in China's total annual energy consumption. Due to the structural characteristics of China's energy resources of "rich in coal, short of oil and gas", coupled with the sloppy mode of economic growth led by secondary industry and the relatively backward energy utilization technology, China's energy consumption structure has been unreasonable for a long time, and the dependence on coal for social development is very high, but the coal combustion can produce a large number of pollutants, including but not limited to sulfur dioxide, nitrogen oxides, carbon monoxide, and soot ($PM_{2.5}$, PM_{10}). Among all pollutants, $PM_{2.5}$ is the main pollutant in Mid-Eastern China, which is a serious hazard to the regional ecological environment and human health (Ma et al., 2022; Chen et al., 2019; Tao et al., 2014; Pope et al., 2011; Hoek et al., 2013). Every 10 % increase in atmospheric $PM_{2.5}$ concentration is associated with a 15–27 % increase in lung cancer (Turner et al., 2011). Outdoor air pollution caused by $PM_{2.5}$ causes 3.3 million premature deaths worldwide each year (Lelieveld et al., 2015). As a result, the Chinese government revised ambient air quality standards in 2012 (Li et al., 2016), added $PM_{2.5}$ and other air pollutants, and gradually established a nationwide network of air quality monitoring stations, thus strengthening the monitoring and management of $PM_{2.5}$ and other pollutants (Song et al., 2017). Studies have shown $PM_{2.5}$ concentrations in most cities have decreased significantly after 2012 (Xue et al., 2006), indicating that the Chinese government's monitoring and treatment measures have had a positive effect.

* Corresponding author.
E-mail addresses: zhangyj@whu.edu.cn (Y. Zhang), ones_w@whu.edu.cn (W. Wu), 3234902193@qq.com (Y. Li), yansheng.li@whu.edu.cn (Y. Li).

https://doi.org/10.1016/j.envint.2023.107941
Received 25 January 2023; Received in revised form 24 March 2023; Accepted 17 April 2023
Available online 20 April 2023

The 2019 novel coronavirus (COVID-19) is a major international natural disaster that erupted at the end of 2019, its outbreak has had an extremely profound impact on the entire world. In China, the COVID-19 outbreak coincided with the Chinese Lunar New Year, the population movement at this time was much higher than usual, which provided favorable conditions for the rapid spread of COVID-19. To curb the spread of COVID-19, China took the initiative to blockade Wuhan, and various local governments also carried out strong control measures to reduce the travel and gathering of people, and the results showed that these measures were very effective (Kraemer et al., 2020). The closure or control of shopping malls, factories, and other places, which reduced $PM_{2.5}$ production at the source, led to a decrease in atmospheric $PM_{2.5}$ concentrations. Chauhan et al. showed that Beijing and Shanghai, which started their blockade in mid-February 2020, both had 50 % lower $PM_{2.5}$ concentrations in March than in February (Chauhan and Singh, 2020). Chu et al. found that the strict control measures and social blockade for COVID-19 outbreak prevention and control led to a decrease in $PM_{2.5}$ concentrations in Wuhan, Hubei (excluding Wuhan) and China (excluding Hubei) by 35 %, 29 % and 19 % (Chu et al., 2021).

Studies show that $PM_{2.5}$ concentration is a gold indicator for environmental monitoring and social science research, which is closely related to human social life (Li et al., 2001; Geng et al., 2018; Xue et al., 2019; Xiao et al., 2020; Stowell et al., 2019; Zhang et al., 2020). However, the number of monitoring stations is very limited, making it difficult to conduct a high spatial density investigation. As a result, using remote sensing inversion techniques to explore a high spatial density $PM_{2.5}$ concentration change investigation method is very important and concerning. But the relationship between $PM_{2.5}$ concentration and elements is nonlinear and difficult to represent by mathematical formulae. Deep learning algorithms are well known to handle nonlinear relationships, and many scholars have done some research in this area (Wang et al., 2022; Kitsiou and Karydis, 2011; Yuchi et al., 2022), so using deep learning algorithms to invert $PM_{2.5}$ concentration is an option. Studies by many scholars have shown that deep neural networks (DNN), convolutional neural networks (CNN), recurrent neural networks (RNN), and long short-term memory networks (LSTM) have good performance in $PM_{2.5}$ concentration inversion (Wang and Sun, 2019; Zamani et al., 2019; Yan et al., 2020; Qin et al., 2019; Tong et al., 2019). There is a strong correlation between aerosol optical thickness (AOD) and $PM_{2.5}$ concentration, but considerable uncertainty exists when only AOD is used to retrieve $PM_{2.5}$ (Li et al., 2017). To enhance the inversion, scholars have added other relevant elements to the model, such as meteorological elements (temperature, humidity, surface pressure, etc.), vegetation cover elements, elevation elements, population and road elements, and time elements (Li et al., 2017; Xu et al., 2020; Yan et al., 2021).

In this study, we use 12 types of multi-source data such as AOD, temperature, humidity, boundary layer height, and vegetation cover as inversion factors. Because the deep learning models are good at learning the nonlinearity relationship between $PM_{2.5}$ and factors, we use a modern deep learning model to invert $PM_{2.5}$ concentrations in Mid-Eastern China. Finally, we realize a high spatial density $PM_{2.5}$ concentration change investigation method, and analyze the spatial and temporal changes of $PM_{2.5}$ concentrations from 2016 to 2021. This time period not only covers the whole process of the COVID-19 outbreak in China from zero to outbreak to remission, but also covers a long period of time before the COVID-19 outbreak, which can help us understand the trend of PM2.5 concentration change in the study area normally. We investigate the effects of control measures on $PM_{2.5}$ concentrations before and after the COVID-19 epidemic period, and find that $PM_{2.5}$ concentrations change in Mid-Eastern China before and after the COVID-19 outbreak have the following characteristics:

- Seasonal differences in $PM_{2.5}$ concentrations are pronounced, with the highest concentrations in winter, the second highest in autumn and the lowest in summer. However, high $PM_{2.5}$ concentrations at different seasons are mainly found in the North China Plain, which is heavily polluted by heavy industry.
- The spatial distribution of annual mean $PM_{2.5}$ concentrations is closely related to secondary industry, economic development, and physical geographic features. In terms of temporal distribution, annual mean $PM_{2.5}$ concentration in most areas is decreasing year-on-year, and annual mean $PM_{2.5}$ concentration in the region declined significantly in 2020.
- According to our experimental results, when China's COVID-19 lockdown policy is at its strictest, the reduction in annual mean PM2.5 concentration in many provinces in the region show a positive correlation with the proportion of secondary industry in GDP. Although China's epidemic situation in 2021 is patched up, annual mean PM2.5 concentrations rebound weakly in these provinces.

2. Materials

2.1. Study area

The study area of this paper is Mid-Eastern China (Taiwan Province is excluded due to the lack of data from Taiwan Province), and the whole area contains 10 provincial administrative units, such as Beijing, Tianjin, Hebei, and Shandong. Fig. 1 shows the geographic location of the study area and the distribution of air quality monitoring stations. The numerous air quality monitoring stations provide a database for the development of air environment management regulations and policies in the region. Meanwhile, according to the China Statistical Yearbook (2021) and the Statistical Table of Administrative Divisions of the People's Republic of China (2020) (National Bureau of Statistics of China, 2021; Ministry of Civil Affairs of China. Statistical Table of Administrative Divisions of China., 2020), the 10 provincial administrative units in the study area account for 46.64 % of China's GDP, 10.53 % of China's total area, and 37.83 % of China's total population. This region is a very important area in China due to its good location and economic development, which continues to attract a large influx of people. But the developed economy, dense population, and high industrialization also make the overall air quality in this region poor. Since 2012, China has increased its efforts to monitor and control air pollutants, which has improved ambient air quality. Government control measures in response to COVID-19 have also affected pollutant emissions to some extent. Therefore, understanding the overall trend of $PM_{2.5}$ concentrations in the region in recent years and the changes in $PM_{2.5}$ concentration during the 2020 epidemic closure period are important for residents' health, environmental protection, and development policy formulation.

2.2. Experiment data

2.2.1. $PM_{2.5}$ concentration data

$PM_{2.5}$ concentration data are provided by the China Air Quality Historical Data website (https://quotsoft.net/air/), which is derived from air quality monitoring stations distributed nationwide. As of 2021, there are more than 2,000 monitoring stations nationwide. Monitoring stations measure and record local hourly concentrations of $PM_{2.5}$, PM_{10}, SO_2, NO_2, O_3, CO, and process them to obtain hourly pollutant concentrations, 24-hour mean sliding concentrations, and the Air Quality Index (AQI). Data are then uploaded to the China National Environmental Monitoring Center (CNEMC, https://www.cnemc.cn/) and published in real time on the National Urban Air Quality Platform. Currently available $PM_{2.5}$ concentration data are available as early as 2013. However, the AOD product used in this study does not have complete annual data until 2016, so the time span for the data in this study was determined to be January 1, 2016 to December 31, 2021.

2.2.2. Himawari-8 AOD data

The Himawari-8 satellite is a geosynchronous satellite launched by

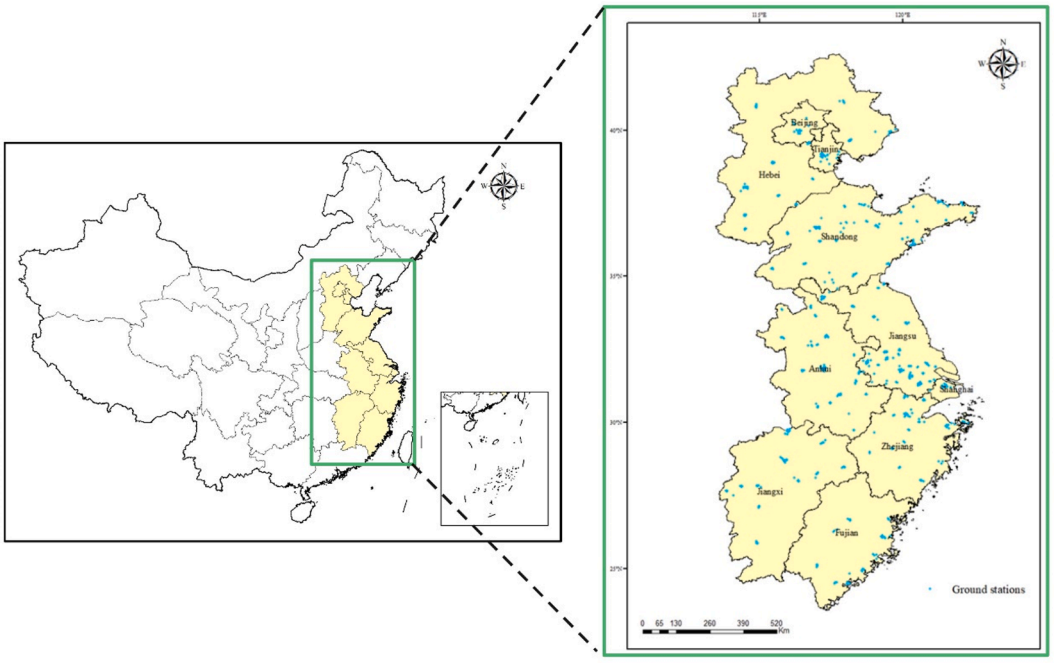

Fig. 1. Mid-Eastern China and its monitoring sites distribution.

the Japan Meteorological Agency at Tanegashima Space Center on October 7, 2014, and officially announced its data in July 2015. The satellite carries an Advanced Himawari Imager (AHI) sensor with 16 bands (including 3 visible bands, 3 near-infrared bands and 10 infrared bands ranging from 0.47 μm to 13.3 μm). The Himawari-8 satellite scans the entire East Asia region every ten minutes, and this scanning method effectively reduces the influence of clouds, which makes more effective data and can reflect the daily distribution of aerosols in East Asia more accurately, providing an option for more refined aerosol monitoring. Current research on the application of Himawari-8 data is mainly focused on cloud top characterization, $PM_{2.5}$ concentration inversion, and fire monitoring (Min et al., 2020; Xu et al., 2017; Xue et al., 2020). The Himawari-8 AOD data products available today can be classified mainly into L2 and L3 data depending on the algorithms used, and L3 data is used in this study.

2.2.3. ERA5 reanalysis information

Many research results have shown that the introduction of meteorological elements can significantly improve the effectiveness of the AOD-$PM_{2.5}$ inversion model, so the reanalysis data from the European Centre for Medium-Range Weather Forecasts (ECMWF) are included in this study. The latest data released by the ECMWF analysis center is the ERA5 reanalysis data, which contains global climate and weather reanalysis data from 1979 to the present, with a temporal resolution of 1 h, a spatial resolution of 0.25°, and an update frequency of one day. In this study, a total of six meteorological factors are selected from the ERA5 reanalysis data: air temperature (T), dew point temperature (DT, used to calculate relative humidity RH), surface pressure (SP), eastward component of wind at a height of 10 m from the surface (U10), northward component of wind at a height of 10 m from the surface (V10) and atmospheric boundary layer height (PBLH). Considering that surface vegetation also has a certain degree of influence on $PM_{2.5}$ concentration, two vegetation cover elements, high vegetation cover index (HVC) and low vegetation cover index (LVC), are also selected.

2.2.4. Elevation data and time data

This paper uses a 30-m resolution digital elevation model (DEM) with data from the Shuttle Radar Topographic Mapping Mission (SRTM), an aerospace mapping mission jointly conducted by NASA, the National Mapping Agency (NIMA) of the Department of Defense, and the German and Italian space agencies. At the same time, considering that $PM_{2.5}$ concentration has obvious time-varying characteristics, and this paper involves a large time span of the study. Therefore, we transform the dates of the data into days and months, and then add them to the inversion as temporal data.

3. Method

Although there is a strong correlation between aerosol optical thickness (AOD) and $PM_{2.5}$ concentration, $PM_{2.5}$ is often influenced by multiple factors (meteorological elements, vegetation cover elements, elevation elements, population and road elements, and temporal elements, etc.) at the same time (Li et al., 2017; Xu et al., 2020; Yan et al., 2021). Therefore, in addition to the AOD factor, meteorological factors such as temperature and humidity, vegetation cover factor, elevation factor, and time factor are also considered in this paper. The correlation between each factor and $PM_{2.5}$ concentration is shown in Fig. 2, which shows a strong nonlinear relationship between $PM_{2.5}$ and the factors.

Nowadays, deep learning algorithms are widely used in the concentration inversion of air pollutants because they can better capture the characteristics of independent variables and approximate nonlinear functions of arbitrary complexity with arbitrary accuracy. Ordinary statistical regression models are not suitable for such complex nonlinear relationships of multiple elements, and deep learning algorithms are a new option to solve such problems, which has been confirmed by many scholars' studies. For example, Gupta et al. estimated $PM_{2.5}$ concentrations using a neural network model based on three years of MODIS AOD and meteorological data in the southeastern United States, and the regression coefficient of the estimated results reached 0.74, which is higher than simple linear regression and multiple regression, verifying the feasibility and potential of using neural networks for air quality monitoring (Gupta and Christopher, 2009). Li et al. proposed a deep convolutional neural network (CNN) model to learn the relationship between population, gross domestic product (GDP), topography, land use, land cover, and $PM_{2.5}$ to achieve a highly accurate spatial estimation of $PM_{2.5}$ (Li et al., 2019). Lee et al. used the Korean Peninsula as the research area and used GOCI's TOA reflectance data and meteorological reanalysis data to retrieve the ground $PM_{2.5}$ concentrations in this area

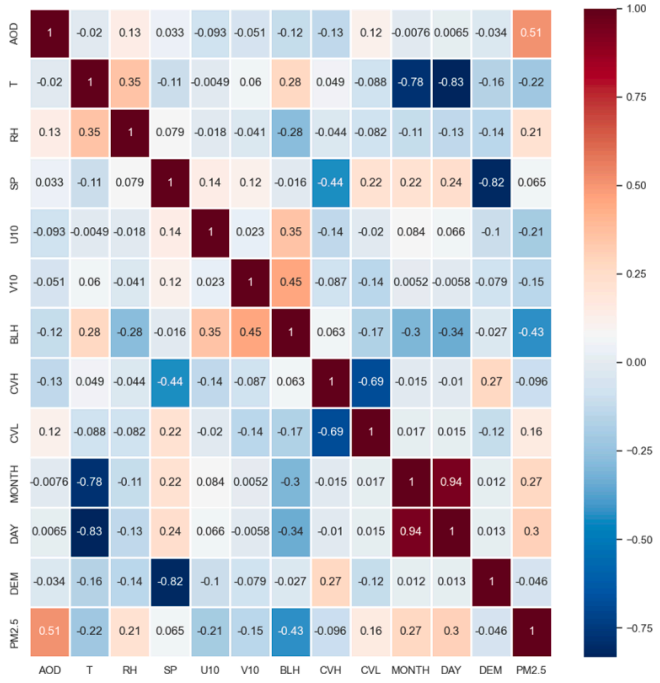

Fig. 2. Correlation between inversion factors and $PM_{2.5}$ concentration.

through the DNN model. Compared to traditional random forest and multiple linear regression models, DNN can more effectively reflect spatial characteristics of $PM_{2.5}$ in the Korean Peninsula (Lee et al., 2021).

Therefore, inspired by previous studies, in order to learn the nonlinearity relationship between $PM_{2.5}$ and input factors preferably, we use the deep neural network (DNN) for $PM_{2.5}$ concentration inversion in this study. The input data of the model input layer is a 12-dimensional vector corresponding to each pixel (containing 12 multi-source inversion factors such as aerosol optical thickness, temperature, relative humidity, surface pressure, and atmospheric boundary layer height). There are four hidden layers in our DNN model, and the number of neurons in each layer is set to 1000, 700, 400 and 100 respectively, and finally the $PM_{2.5}$ concentration inversion value of each pixel is output by the output layer. Combining the input features, the model's forward data flow graph is shown in Fig. 3.

In our model, each hidden layer is made up of two sublayers, a fully connected layer (FC) connects the model's input or the output of the previous hidden layer, then the output of the FC layer passes through a rectified linear unit (ReLU) activation function layer, and finally the output of the ReLU layer inputs the next FC layer or output layer. In the hidden layer, we choose ReLU function as our model's activation function, because the range of ReLU function is $[0, \infty)$, it can not only overcome the problem of saturation and vanishing gradient (Nair and Hinton, 2010), but also better match the numerical characteristics of atmospheric pollution concentration. The forward operation of each hidden layer can be described as:

$$x_i^{k+1} = W_i^{k+1} Y^k + b_i^{k+1} \tag{1}$$

$$Y_i^{k+1} = f\left(x_i^{k+1}\right) \tag{2}$$

where k is the index of the hidden layer; Y^k is the vector of outputs from hider layer k, and the vector of inputs into layer $k+1$; W^k and b^k are the weights and biases of layer k, respectively. The f (•) function is the ReLU activation function.

Furthermore, to prevent overfitting, we use Dropout technology in our deep learning model. Dropout has been shown to significantly reduce overfitting and improve neural network performance (Srivastava et al., 2014). For the loss function, because the $PM_{2.5}$ concentration prediction task is a nonlinear regression problem, we select mean square error (*MSE*) as our loss function. *MSE* is formulated as follows:

$$MSE = \frac{1}{n}\sum_{i=1}^{n}(\hat{y}_i - y_i)^2 \tag{3}$$

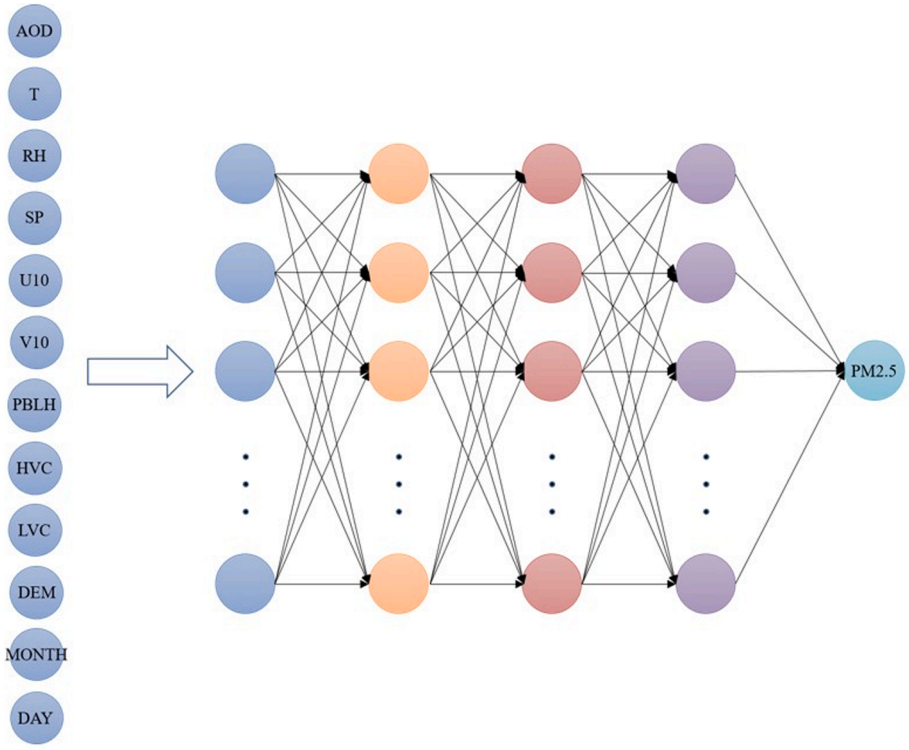

Fig. 3. Forward data flow graph of our model.

where n is the number of data, $\widehat{y}_i$ is the $PM_{2.5}$ concentration obtained from the model inversion, y_i is the true $PM_{2.5}$ concentration. Adamax optimizer is chosen as the optimizer for our model training, which has better performance and high iteration efficiency (Kingma and Ba, 2014).

4. Experimental results

4.1. Model performance

Based on $PM_{2.5}$ data from monitoring stations in the study region, it can be found that $PM_{2.5}$ concentrations have more obvious seasonal differences. Therefore, when using the DNN model to invert $PM_{2.5}$ concentrations, we model them by season. The data is divided into four datasets according to their seasons, and then each dataset is randomly sampled 80 % of the data form the training dataset and the remaining 20 % form the test dataset.

Two evaluation metrics, coefficient of determination (R^2) and root mean square error (*RMSE*), are used to evaluate the performance of the model on the test set, both of which are formulated as follows:

$$R^2 = 1 - \frac{\sum_i (\widehat{y}_i - y_i)^2}{\sum_i (y_i - \overline{y})^2} \tag{4}$$

$$RMSE = \sqrt{\frac{1}{n}\sum_{i=1}^{n} (\widehat{y}_i - y_i)^2} \tag{5}$$

In the formula, $\widehat{y}_i$ is the $PM_{2.5}$ concentration obtained from the model inversion, y_i is the true $PM_{2.5}$ concentration and $\overline{y}$ is the mean value of $PM_{2.5}$ concentration.

After determining the model, datasets, activation function, loss function, optimizer, and evaluation metrics, we tune the hyper-parameters through several experiments and finally obtain the detailed parameter settings of the model as shown in Table 1.

The model is trained with data from different seasons to learn the characteristics of $PM_{2.5}$ concentrations in four seasons. Table 2 shows the evaluation metrics of the DNN model when inverting $PM_{2.5}$ concentrations on different seasonal datasets. It can be seen that the model can achieve a coefficient of determination above 0.83 and up to 0.919 in all four training sets, while it stays above 0.75 in each seasonal test set. The inverse effect of the test set varies widely among seasons. In spring, autumn and winter, the R^2 of the model is beyond 0.8, while the R^2 in summer is only 0.753, indicating that the situation is more complicated in summer compared with other seasons, and the explanatory power of the model is slightly insufficient, and further optimization of the model or consideration of the influence of other factors on $PM_{2.5}$ concentration is needed. The root mean square errors of the four test sets in spring, summer, autumn and winter are 12.336 μg/m^3, 9.152 μg/m^3, 12.627 μg/m^3 and 16.002 μg/m^3, respectively, which are worse than the training set. Although the R^2 and *RMSE* of the model on the test set are slightly worse than those on the training set, they are still within the acceptable range. The values of the two assessment indicators indicate that the model has good applicability in the study area and can solve the problem of inversion of $PM_{2.5}$ concentrations over a large area of the region.

Table 1
Model parameter setting table.

Model content	Specific settings
Number of hidden layers	4
Number of neurons in each hidden layer	1000, 700, 400, 100
Activation functions	ReLU
Loss function	MSE
Optimizers	Adamax
Regularization	Dropout (P = 0.3)
Initial learning rate	0.001
Batch size	256
Epoch	1000

Table 2
Evaluation metrics of the model on different seasonal datasets.

Seasons and dataset types		R^2	*RMSE*(μg/m^3)
Spring	Training set	0.867	9.314
	Test set	0.805	12.336
Summer	Training set	0.835	8.646
	Test set	0.753	9.152
Autumn	Training set	0.904	9.522
	Test set	0.831	12.627
Winter	Training set	0.919	12.322
	Test set	0.809	16.002

4.2. Seasonal-scale $PM_{2.5}$ concentration change from 2016 to 2021

Fig. 4 shows the spatial distribution of the average $PM_{2.5}$ concentrations in the study area for different seasons from 2016 to 2021 obtained from the model inversion. From 2016 to 2021, the region as a whole maintains the worst $PM_{2.5}$ pollution in winter, followed by autumn, with the best air quality in summer and spring in between summer and autumn. Considering the actual characteristics of $PM_{2.5}$ concentration in all seasons, we take 35 μg/m^3 as the standard line of $PM_{2.5}$ concentration, 60 μg/m^3 as high $PM_{2.5}$ concentration, and 90 μg/m^3 as ultra-high $PM_{2.5}$ concentration.

Comparing the spatial distribution of $PM_{2.5}$ pollution in spring of each year, it is easy to see that there is a southward expansion of high $PM_{2.5}$ concentration areas in the southern part of the Beijing-Tianjin-Hebei region and an overall deterioration of the air quality environment in the central part of the study area (i.e., northern Anhui and Jiangsu provinces and southwestern Shandong province). By 2021, a larger area of high $PM_{2.5}$ concentrations emerges in the central part of the study area. It is noteworthy that the $PM_{2.5}$ concentrations in the spring of the study area basically remain around 43 μg/m^3 in all years, indicating that the regional air quality in the spring shows a kind of local variation and overall balance. Summer is the season with the best air quality among the four seasons. $PM_{2.5}$ concentrations in most areas are below 35 μg/m^3, meeting the target of the first transitional phase of the international monitoring standard for $PM_{2.5}$. Only the central and southern parts of Beijing, Tianjin and Hebei have large areas with high $PM_{2.5}$ concentrations. Compared to spring and summer, $PM_{2.5}$ pollution is more severe in autumn, with higher average concentrations across the region and widespread areas of high $PM_{2.5}$ concentrations in the southern provinces where air quality was previously better. $PM_{2.5}$ pollution in winter is extremely serious, with ultra-high $PM_{2.5}$ concentration areas occupying about half of the study area, and the average concentration in some areas is even higher than 120 μg/m^3, and the average winter concentration in the whole region has remained above 60 μg/m^3 for these six years, much higher than in spring, summer and autumn.

In addition, it can also be found that there is some similarity between regions with severe $PM_{2.5}$ pollution in different seasons, and they all tend to contain parts of the North China Plain or the North China Plain (only the south-central Beijing-Tianjin-Hebei region is more polluted in summer), which is related to factors such as heavy industrial pollution emissions in the North China Plain (Yao et al., 2016).

4.3. Interannual scale $PM_{2.5}$ concentration change from 2016 to 2021

Fig. 5 shows the spatial distribution of annual mean $PM_{2.5}$ concentrations in the study area from 2016 to 2021. Annual mean $PM_{2.5}$ concentration is spatially high in the central part and low in the northern and southern ends. Areas with higher $PM_{2.5}$ concentrations in patches are distributed in the north and south ends, while areas with $PM_{2.5}$ concentrations below 35 μg/m^3 are relatively limited. There are three main areas with severe pollution in the central part, namely the south-

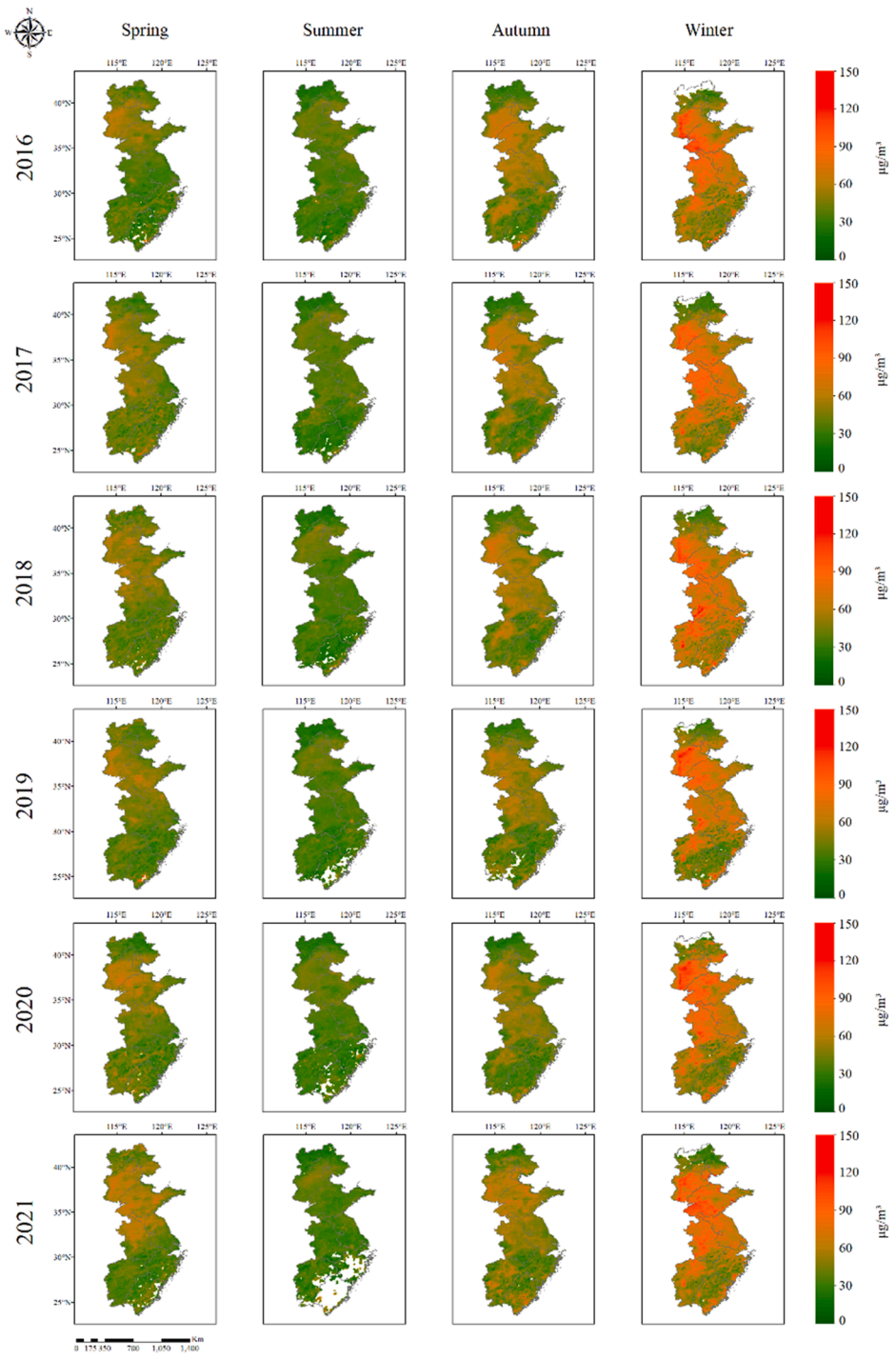

Fig. 4. Spatial distribution of average $PM_{2.5}$ concentrations in four seasons from 2016 to 2021.

central Beijing-Tianjin-Hebei region, Shandong region, and parts of the Yangtze River Delta (mainly Anhui Province and Jiangsu Province).

From 2016 to 2021, air quality in the south-central Beijing-Tianjin-Hebei region is gradually getting better amidst fluctuations. Specific performance is that the area of 60 μg/m^3 and above is decreasing, the area of 45 μg/m^3 and below is expanding, and the peak regional $PM_{2.5}$ concentration is decreasing from 85.5 μg/m^3 to 76.6 μg/m^3. This is due to the presence of mountains in the central part of Shandong, such as Mount Tai and Mount Meng, which are surrounded by the flat topography of the Northwest Lu Plain and the Jiao Lai Plain, and the unique topographic conditions affect the distribution of $PM_{2.5}$ pollution. Air pollution in Shandong is better than that in the south-central Beijing-Tianjin-Hebei region, with an average $PM_{2.5}$ concentration of 3.24 % lower than the latter over the past six years. The northern Yangtze River Delta is not only the less polluted area of $PM_{2.5}$ among the three regions, but also the area with the most significant improvement in air quality. The average $PM_{2.5}$ concentration in the region over the past six years is 53.35 μg/m^3, which is 6.42 % and 3.29 % lower than that in the central and southern Beijing-Tianjin-Hebei and Shandong regions respectively. In 2016 and 2017, more places in the northern Yangtze River Delta had average $PM_{2.5}$ concentrations of 75 μg/m^3. From 2018 to 2020, the areas with concentrations of 75 μg/m^3 decreased significantly, and areas with concentrations of 45 μg/m^3 increased. By 2021, pollution in the northern Yangtze River Delta is increasing, but it is still better than in 2016.

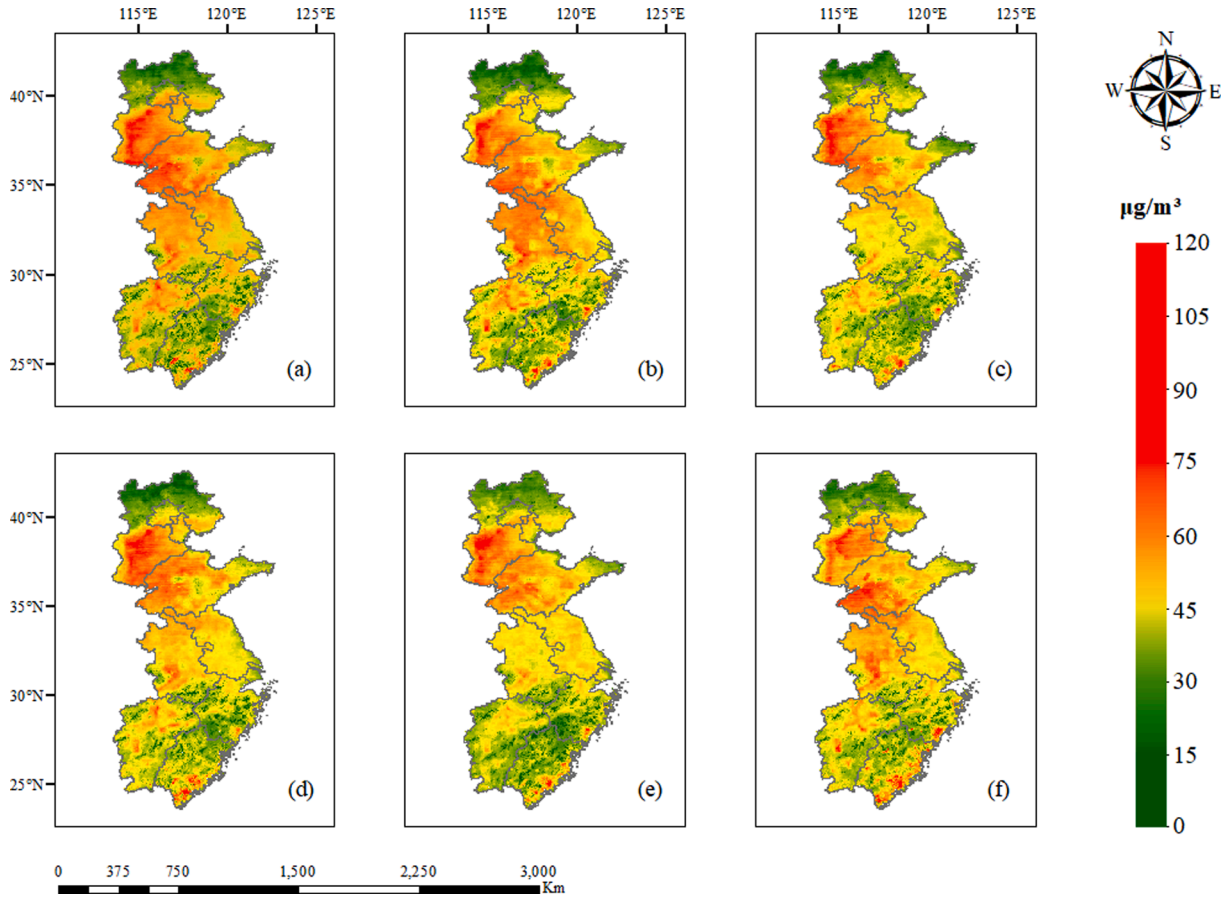

Fig. 5. Spatial distribution of annual average $PM_{2.5}$ concentrations from 2016 to 2021.

In general, air quality in the north and south ends of the study area barely meets international standards, and air quality in the central region is gradually improving overall, but is still far from international standards. The gradual improvement in air quality is consistent with the past study (Xue et al., 2006), indicating that the Chinese government's monitoring and treatment measures have had a positive effect.

Fig. 6 shows the changes in $PM_{2.5}$ concentrations for the entire region in 2020 and 2021 compared to the previous year. As a result of COVID-19, different levels of control measures were taken from late January to early April 2020, which had a dampening effect on $PM_{2.5}$

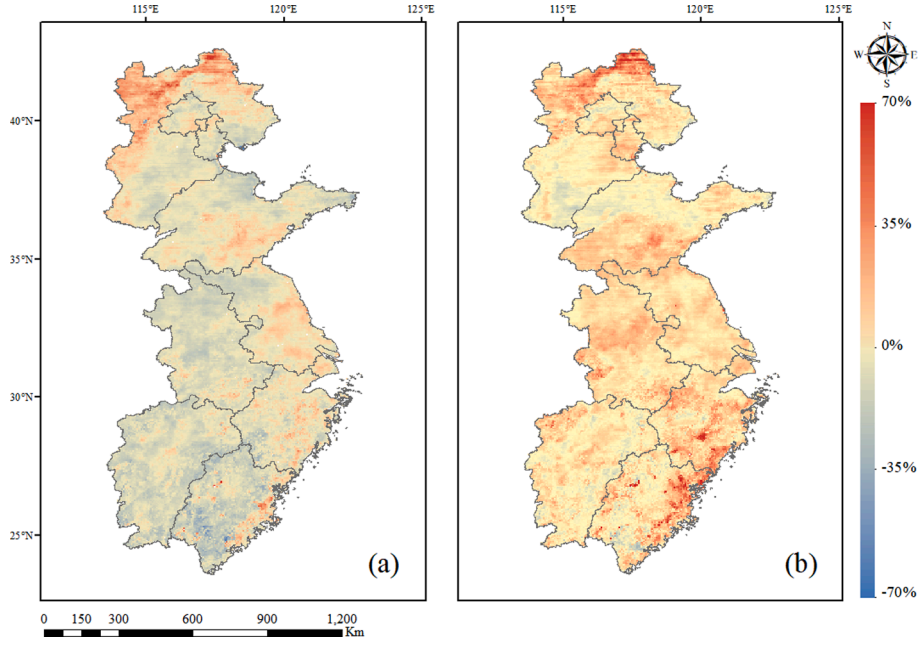

Fig. 6. Relative change in annual average $PM_{2.5}$ concentration.

concentrations. According to Fig. 6a, the percentage decrease in 2020 reaches more than 35 % in a small part of the study area and ranges from 5 % to 20 % in most areas, which is very similar to what chu et al found (Chu et al., 2021). The average decrease in $PM_{2.5}$ concentration for the whole year is 3.07 % compared to the previous year; and the average percentage decrease was higher than the 1 % decrease in 2019, confirming the suppressive effect of epidemic control measures on $PM_{2.5}$ concentration. In 2021, the COVID-19 in China eases, nearly 80 % of the study region $PM_{2.5}$ concentrations are elevated, with the remaining 20 % experiencing more limited percentage declines concentrate in the 0 % to 10 % range. With $PM_{2.5}$ concentrations increasing in most areas, $PM_{2.5}$ concentrations in the study area increase by an average of 9.8 % throughout the year, with overall $PM_{2.5}$ pollution levels better than in 2019 before the epidemic but worse than in 2020.

4.4. $PM_{2.5}$ concentration changes during the closure control period from 2019 to 2021

Based on the global $PM_{2.5}$ concentrations obtained from the inversion, the first two sections analyze the spatial and temporal variation characteristics of $PM_{2.5}$ concentrations in the whole study area before and after COVID-19 outbreak from the seasonal and annual perspectives, and focus on the magnitude of COVID-19′s effect on $PM_{2.5}$ concentrations. After the outbreak, strong control measures were taken in mainland China, which led to a gradual return to normal residential life and business production after several months. The impact of control measures on $PM_{2.5}$ concentrations is undeniable, and how $PM_{2.5}$ concentrations changed during the control period is an issue worth exploring. This section examines PM2.5 concentrations in each province and region for the same period from 2019 to 2021, using the closure of Wuhan as the study period. Although the implementation of control measures was not exactly same in each province of the study area, and the industrial structure of different provinces varies considerably, this period in 2020 was the period of the massive COVID-19 outbreak in Mid-Eastern China, and the largest number of cities in the study area were closed (He et al., 2020). In addition, if we take the year as the unit of study here, the comparative effect of the experimental results will be weakened because the epidemic situation in China is under control in the second half of 2020.

Fig. 7 shows the variation of the regional average $PM_{2.5}$ concentrations in the study area for the first four months of 2019 to 2021. It can be seen that $PM_{2.5}$ concentrations show an overall decreasing trend from January to April of each year, with January data being significantly higher than the other three months, which is consistent with the seasonal $PM_{2.5}$ characteristics previously obtained. $PM_{2.5}$ concentration is also decreasing year-on-year outside the closure control period (non-grey areas in the figure), which is related to the long-implemented air quality monitoring treatment (Liu et al., 2021). At the same time, the decrease in $PM_{2.5}$ concentration in 2020 compared to the previous year is significantly higher than the decrease in 2021. This is somewhat related to the initiative of “not returning home unless necessary, spend the New Year in the same place”. This initiative is proposed by local governments to reduce the mass movement of people during the Spring Festival in the face of the severe and complex winter epidemic prevention and control situation. The decrease in $PM_{2.5}$ concentration was evident during the period of city closure and control (Chauhan and Singh, 2020). According to the results, the average $PM_{2.5}$ concentration during this period in 2019 is 53.7 $\mu g/m^3$, while the concentration during the same period in 2020 is only 40.53 $\mu g/m^3$, a decrease of 24.53 % in average concentration and 49.11 % in maximum. In the same period of 2021, without the impact of the city closure measures, society basically returns to normal, and the average $PM_{2.5}$ concentration reaches 45.12 $\mu g/m^3$, an increase of 11.32 %, with a maximum increase of 61.07 %. In the face of the sporadic existence of epidemics, small-scale control measures are still implemented in various regions, which to a certain extent changes the production and living patterns of the society and subsequently has an impact on $PM_{2.5}$ concentrations.

The relative changes of the average $PM_{2.5}$ concentrations in 2020 and 2021 during the city closure period are calculated in terms of provinces, and Fig. 8 and Fig. 9 are obtained. As can be seen from Fig. 8a and Fig. 9a, the control measures taken in the face of the epidemic had a significant impact on $PM_{2.5}$ concentrations in the provinces, with all provinces and municipalities in the study area reducing $PM_{2.5}$ concentrations by more than 10 %. Among the three industries, the secondary industry has the greatest impact on $PM_{2.5}$ concentration and is one of the main drivers of its change (Wang et al., 2014). Provinces with a larger share of the secondary sector economy also tend to see their $PM_{2.5}$ concentrations fall more, for example, Jiangsu Province, Zhejiang Province and Anhui Province all saw their $PM_{2.5}$ concentrations fall by more than 30 %. At the same time, it can also be found that the $PM_{2.5}$ concentration in Beijing, where the control measures are very strict but the secondary industry accounts for a relatively low percentage, only

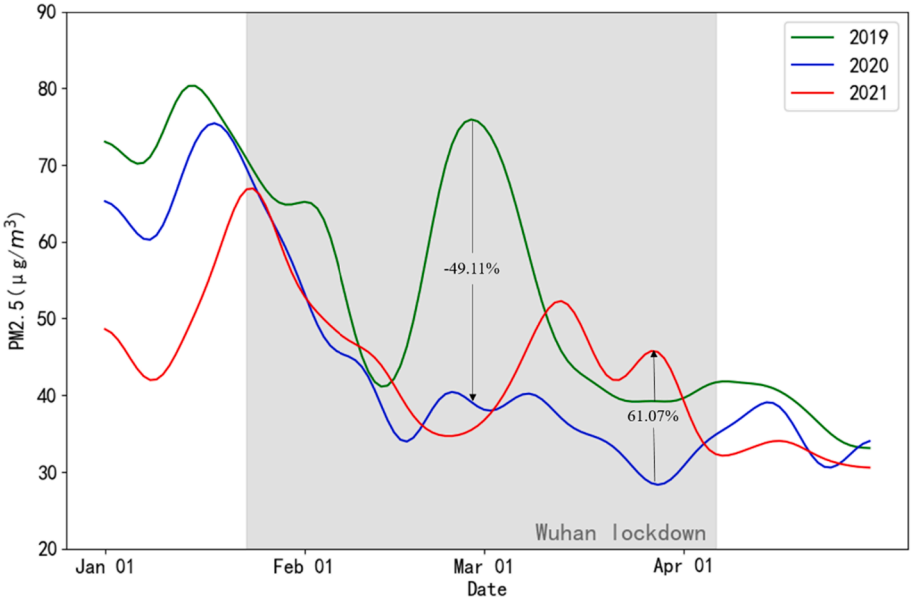

Fig. 7. Change in average $PM_{2.5}$ concentration in the first four months of 2019–2021.

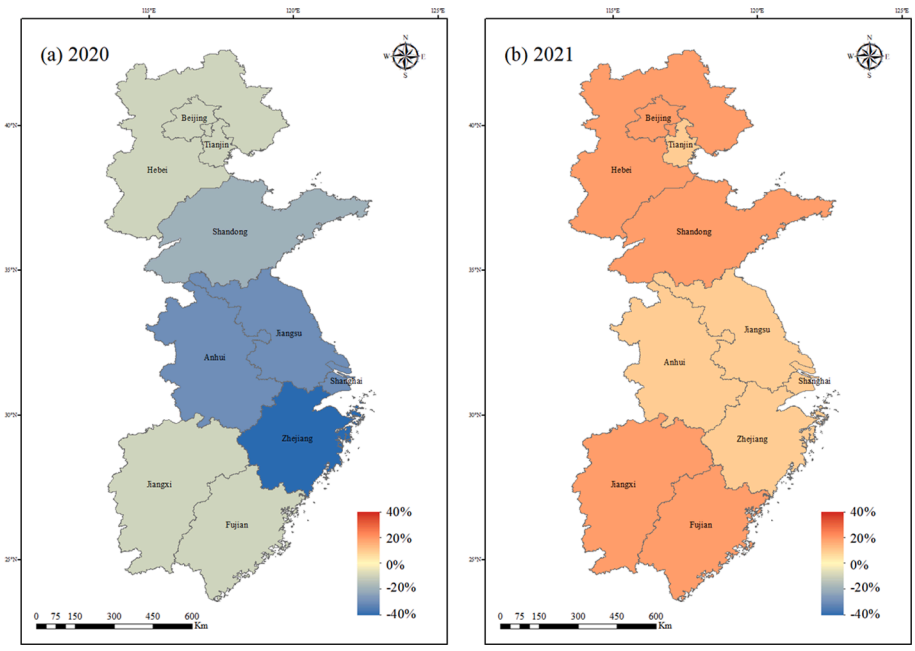

Fig. 8. Relative change in $PM_{2.5}$ concentration by province.

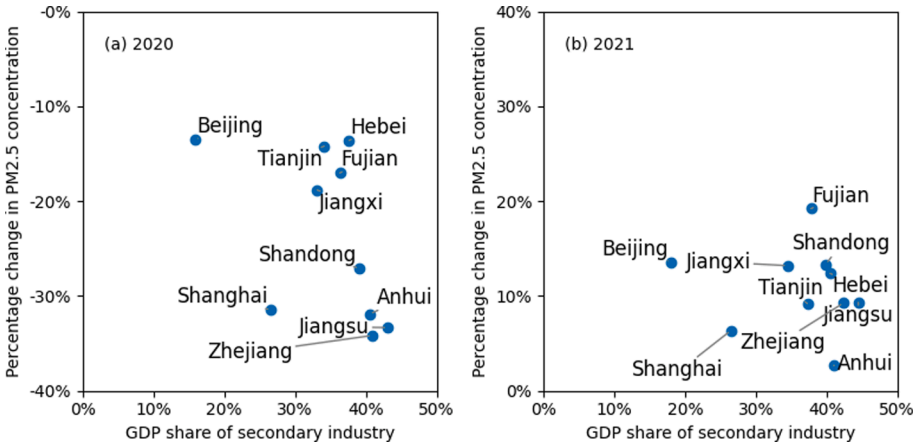

Fig. 9. Relative percentage change in $PM_{2.5}$ concentration by province and share of secondary sector GDP.

decrease by 13.51 %, which also reflects that the secondary industry is a very important source of $PM_{2.5}$. In 2021, there is basically no large-scale epidemic in mainland China, industries are gradually recovering in various regions, and $PM_{2.5}$ concentrations rebound significantly compared to last year's closure period (Fig. 8b). As can be seen from Fig. 9b, majority of provinces have a limited rebound in $PM_{2.5}$ concentrations, concentrated at around 10 %, which is only slightly higher than during the epidemic closure period. Among the provinces with a high share of secondary industry, only Fujian has a recovery of $PM_{2.5}$ concentrations close to 20 %. Therefore, China's epidemic prevention policies have had a huge impact on the secondary industry when the COVID-19 epidemic was very severe, the government should pay more attention to the impact of the epidemic on secondary industry and ensure healthy socio-economic growth during the COVID-19 epidemic prevention and management.

5. Discussion

Although the relationship between COVID-19 and changes in pollutant concentrations has become a hot research topic in environmental science in recent years, there are still many shortcomings in these studies. Many of the studies cover large areas, they investigate the whole world or all of China (Chauhan et al., 2020; Venter et al., 2020; Rodríguez-Urrego and Rodríguez-Urrego, 2020; Wei et al., 2023); but the density of investigations in these works is low due to the high workload. At the same time, there are many studies that focus on individual cities and do not consider regional characteristics (Zoran et al., 2020; Zhang et al., 2023; Jin et al., 2023); so our study is more scientific in spatial scope. In addition, most of these studies use direct measurement data or linear models to investigate, without considering high spatial densities or nonlinearities. In many studies, the learning period is short. For example, Wei et al. only compared and analyzed changes in $PM_{2.5}$ concentration from January to June 2019 and 2020 in mainland China (Wei et al., 2023). These studies did not conduct sufficient comparative studies before; during and after the outbreak. Our work can be said to be the first comprehensive investigation of $PM_{2.5}$ concentration changes in Mid-Eastern China before and after the COVID-19 outbreak with a high spatial density nonlinear investigation method.

In this paper, we use multi-source data and deep learning techniques to investigate $PM_{2.5}$ concentrations. Due to the large scope and time

span of our investigation, which requires a large computational cost. To improve computational efficiency, we build a relatively simple deep learning model. This model is similar to the EntityDenseNet constructed in 2020 by Yan et al. (Yan et al., 2020). Yan et al. also demonstrated that this type of structure outperforms other machine learning algorithms such as backpropagation neural network, extreme gradient boosting, light gradient boosting machine and random forest in the field of $PM_{2.5}$ concentration prediction.

At the same time, we pay more attention to the choice of variables to avoid the loss of prediction accuracy caused by our simple model. In addition to the basic AOD data, we consider various types of factors: meteorological factors such as temperature and humidity, natural factors such as vegetation cover, digital elevation model, and temporal factors. These factors are high spatial density data that can be obtained by remote sensing satellites, while many scholars have only used AOD data and machine learning techniques to invert regional $PM_{2.5}$ concentrations (Chen et al., 2019; Yan et al., 2020; Di et al., 2019; Park et al., 2020; Lu et al., 2021; Just et al., 2018; Harishkumar et al., 2020; Sun et al., 2019; Bagheri, 2022; Pu and Yoo, 2021; Chen et al., 2018). After considering more factors related to $PM_{2.5}$ concentration and obtaining these high spatial density satellite remote sensing data, we combine $PM_{2.5}$ concentration data from ground monitoring stations for supervised training and then use the trained model and these satellite remote sensing data for prediction. Finally, we achieve a high spatial density prediction of $PM_{2.5}$ concentration with high efficiency and accuracy.

It is worth noting that Li et al. used the deep learning model (GTW-GRNN) and AOD data to invert $PM_{2.5}$ concentrations in China, and the best R^2 obtained by this work is 0.80 (Li et al., 2020). Meanwhile, the mean R^2 of the four seasons obtained by our method is also about 0.80, which is very close to GTW-GRNN. At the methodological level, our method can be seen as a simplification of the GTW-GRNN model. The GTW-GRNN model uses a spatiotemporal weighting scheme to improve the accuracy of the simple model for $PM_{2.5}$ concentration inversion in a single grid. This process requires complex calculations. In our method, seasonal features are introduced by adding temporal variables, and spatial features are added by meteorological factors and digital elevation model. Therefore, our method can be considered as an alternative to complex calculations using multi-source features.

This study serves as a good reference for similar regions to formulate corresponding environmental protection and social policies in the event of a major sudden disaster, and provides a comprehensive template for inversion of air pollutant concentrations using multi-source remote sensing data. Meanwhile, to improve the inversion efficiency, we explore the use of multi-source data to simplify the computational process of the complex prediction model. In contrast to previous results, we find that simple models can also perform well after using multi-source data, which was also rarely attempted in previous works. In future work, we can consider combining more multi-source data by using ensemble learning and improving the computational efficiency of complex machine learning models, thus efficiently achieving higher R^2 and more reliable inversion results.

6. Conclusions

We conduct continuous $PM_{2.5}$ concentration inversions for selected regions of China using remotely sensed AOD data products and other reanalysis element data, and analyze spatial and temporal variation characteristics of $PM_{2.5}$ concentrations in the study area during seasons and years based on inversion results before and after the COVID-19 outbreak, and analyze the effects of closure and control measures on $PM_{2.5}$ concentrations throughout the region and in each province during the severe epidemic period. The R^2 of the DNN model uses in this paper is maintained above 0.75, and the *RMSE* on the four seasonal test sets of $PM_{2.5}$ are 12.336 μg/m^3, 9.152 μg/m^3, 12.627 μg/m^3, and 16.002 μg/m^3, respectively. These all indicate that the model and the selected variables can explain the variation in $PM_{2.5}$ concentrations well. Based on the results of this investigation, the following summarizes can be drawn.

From 2016 to 2021, $PM_{2.5}$ concentrations in the study area maintain the seasonal characteristics of the most severe $PM_{2.5}$ pollution in winter, followed by autumn, the best air quality in summer, and spring between summer and autumn. Among them, the regional air quality in spring show a kind of local variation and overall balance ($PM_{2.5}$ concentration increases in some areas, but the regional average concentration is basically maintained at 43 μg/m^3). High $PM_{2.5}$ concentrations at different seasons are mainly found in the North China Plain, which is polluted by heavy industry.

Annual mean $PM_{2.5}$ concentrations in the study area are spatially characterized by high concentrations in the central part and low concentrations at the north and south ends. The $PM_{2.5}$ concentrations at the north and south ends basically meet international standards, while $PM_{2.5}$ pollution is more serious in the central part, and the regions with more prominent pollution contain the south-central Beijing-Tianjin-Hebei region, Shandong region and parts of the Yangtze River Delta. The air quality in the three regions is gradually improving, and the government still needs to pay more attention to it while maintaining the air quality in other regions.

According to results, because of the control measures during the severe epidemic, the annual average $PM_{2.5}$ concentration in the study area decreases by 3.07 % in 2020, while the annual average $PM_{2.5}$ concentration rebound by 9.8 % in 2021. During the Wuhan closure period, the average $PM_{2.5}$ concentration decreases by 24.53 % in 2020 and increases by 11.32 % in 2021. Meanwhile, the extent of $PM_{2.5}$ concentration reduction in 2020 varied widely across provinces, some provinces with a large share of the secondary industry decreases by more than 30 %, while Beijing, with strict control measures but a small share of the secondary industry, decreases by only 13.51 %. In 2021, $PM_{2.5}$ concentrations in the provinces rebound slightly, with most provinces rebounding by about 10 %.

Credit author statement

All authors of this research paper have directly participated in the planning, execution, or analysis of the study. All authors of this paper have read and approved the final version submitted. The contents of this manuscript have not been copyrighted or published previously. The contents of this manuscript are not under consideration for publication elsewhere. There are no directly related manuscripts or abstracts, published or unpublished, by any author(s) of this paper.

CRediT authorship contribution statement

Yongjun Zhang: Investigation. **Wenpin Wu:** Writing - original draft. **Yiliang Li:** Writing - original draft. **Yansheng Li:** Methodology.

Declaration of Competing Interest

The authors declare that they have no known competing financial interests or personal relationships that could have appeared to influence the work reported in this paper.

Data availability

Data will be made available on request.

Acknowledgements

This work was supported in part by the State Key Program of the National Natural Science Foundation of China under grant 42030102, the National Natural Science Foundation of China under grant 41971284. and the Fundamental Research Funds for the Central

Universities under grant 2042022kf1201.

References

Bagheri, H., 2022. A machine learning-based framework for high resolution mapping of PM2. 5 in Tehran, Iran, using MAIAC AOD data. Adv. Space Res. 69 (9), 3333–3349.

Chauhan, A., Singh, R.P., 2020. Decline in PM2. 5 concentrations over major cities around the world associated with COVID-19. Environ. Res. 187, 109634.

Chauhan, A., Singh, R.P., 2020. Decline in PM2.5 concentrations over major cities around the world associated with COVID-19. Environ. Res. 187, 109634.

Chen, G., Li, S., Knibbs, L.D., et al., 2018. A machine learning method to estimate PM2. 5 concentrations across China with remote sensing, meteorological and land use information. Sci. Total Environ. 636, 52–60.

Chen, J., Yin, J., Zang, L., et al., 2019. Stacking machine learning model for estimating hourly PM2.5 in China based on Himawari 8 aerosol optical depth data. Sci. Total Environ. 697, 134021.

Chu, B., Zhang, S., Liu, J., et al., 2021. Significant concurrent decrease in PM2.5 and NO2 concentrations in China during COVID-19 epidemic. J. Environ. Sci. 99, 346–353.

Di, Q., Amini, H., Shi, L., et al., 2019. An ensemble-based model of PM2. 5 concentration across the contiguous United States with high spatiotemporal resolution. Environ. Int. 130, 104909.

Geng, G., Murray, N.L., Chang, H.H., et al., 2018. The sensitivity of satellite-based PM2. 5 estimates to its inputs: Implications to model development in data-poor regions. Environ. Int. 121, 550–560.

Gupta, P., Christopher, S.A., 2009. Particulate matter air quality assessment using integrated surface satellite and meteorological products 2 A neural network approach. J. Geophys. Res. 114.

Harishkumar, K.S., Yogesh, K.M., Gad, I., 2020. Forecasting air pollution particulate matter (PM2. 5) using machine learning regression models. Proc. Comput. Sci. 171, 2057–2066.

He, G., Pan, Y., Tanaka, T., 2020. The short-term impacts of COVID-19 lockdown on urban air pollution in China. Nat. Sustain. 3 (12), 1005–1011.

Hoek, G., Krishnan, R.M., Beelen, R., et al., 2013. Long-term air pollution exposure and cardio- respiratory mortality: a review. Environ. Health 12, 43.

Jin, Q., Luo, Y., Meng, X., et al., 2023. Short-and long-term impacts of the COVID-19 epidemic on urban PM2. 5 variations: Evidence from a megacity, Chengdu. Atmos. Environ. 294, 119479.

Just, A.C., De, Carli, M.M., Shtein, A., et al., 2018. Correcting measurement error in satellite aerosol optical depth with machine learning for modeling PM2. 5 in the Northeastern USA. Remote Sens. 10(5), 803.

Kingma, D., Ba, J., 2014. Adam: A Method for Stochastic Optimization. Computer Science.

Kitsiou, D., Karydis, M., 2011. Coastal marine eutrophication assessment: a review on data analysis. Environ. Int. 37 (4), 778–801.

Kraemer, M.U.G., Yang, C., Gutierrez, B., et al., 2020. The effect of human mobility and control measures on the COVID-19 epidemic in China. Science (American Association for the Advancement of Science) 368, 493–497.

Lee, C., Lee, K., Kim, S., et al., 2021. Hourly ground-level PM2.5 estimation using geostationary satellite and reanalysis data via deep learning. Remote Sens. 13, 2121.

Lelieveld, J., Evans, J.S., Fnais, M., et al., 2015. The contribution of outdoor air pollution sources to premature mortality on a global scale. Nature 525, 367–371.

Li, J., Garshick, E., Hart, J.E., et al., 2021. Estimation of ambient PM2. 5 in Iraq and Kuwait from 2001 to 2018 using machine learning and remote sensing. Environ. Int. 151, 106445.

Li, T., Shen, H., Yuan, Q., et al., 2017. Estimating ground-level PM2.5 by fusing satellite and station observations: a geo-intelligent deep learning approach. Geophys. Res. Lett. 44, 11, 911–985, 993.

Li, J., Jin, M., Li, H., 2019. Exploring spatial influence of remotely sensed PM2.5 concentration using a developed deep convolutional neural network model. Int. J. Environ. Res. Public Health 16, 454.

Li, R., Mao, H., Wu, L., et al., 2016. The evaluation of emission control to PM concentration during Beijing APEC in 2014. Atmos. Pollut. Res. 7, 363–369.

Li, T., Shen, H., Yuan, Q., et al., 2020. Geographically and temporally weighted neural networks for satellite-based mapping of ground-level PM2.5. ISPRS J. Photogramm. Remote Sens. 167, 178–188.

Liu, G., Dong, X., Kong, Z., et al., 2021. Does national air quality monitoring reduce local air pollution? The case of PM2. 5 for China. J. Environ. Manage. 296, 113232.

Lu, X., Wang, J., Yan, Y., et al., 2021. Estimating hourly PM2. 5 concentrations using Himawari-8 AOD and a DBSCAN-modified deep learning model over the YRDUA, China. Atmos. Pollut. Res. 12 (2), 183–192.

Ma, P., Tao, F., Gao, L., et al., 2022. Retrieval of fine-grained PM2.5 spatiotemporal resolution based on multiple machine learning models. Remote Sens. 14, 599.

Min, M., Li, J., Wang, F., et al., 2020. Retrieval of cloud top properties from advanced geostationary satellite imager measurements based on machine learning algorithms. Remote Sens. Environ. 239, 111616.

Ministry of Civil Affairs of China. Statistical Table of Administrative Divisions of China, 2020. Available online: http://xzqh.mca.gov.cn/statistics/2020.html.

Nair, V., Hinton, G.E., 2010. Rectified linear units improve restricted Boltzmann machines. ICML. 807–814.

National Bureau of Statistics of China. China Statistical Yearbook 2021, 2021, Available online: http://www.stats.gov.cn/tjsj/ndsj/2021/indexch.htm.

Park, Y., Kwon, B., Heo, J., et al., 2020. Estimating PM2. 5 concentration of the conterminous United States via interpretable convolutional neural networks. Environ. Pollut. 256, 113395.

Pope, C.A., Brook, R.D., Burnett, R.T., et al., 2011. How is cardiovascular disease mortality risk affected by duration and intensity of fine particulate matter exposure? An integration of the epidemiologic evidence. Air Qual. Atmos. Health 4, 5–14.

Pu, Q., Yoo, E.H., 2021. Ground PM2.5 prediction using imputed MAIAC AOD with uncertainty quantification. Environ. Pollut. 274, 116574.

Qin, D., Yu, J., Zou, G., et al., 2019. A novel combined prediction scheme based on CNN and LSTM for urban PM2.5 concentration. IEEE Access 7, 20050–20059.

Rodríguez-Urrego, D., Rodríguez-Urrego, L., 2020. Air quality during the COVID-19: PM2. 5 analysis in the 50 most polluted capital cities in the world. Environ. Pollut. 266, 115042.

Song, C., Wu, L., Xie, Y., et al., 2017. Air pollution in China: Status and spatiotemporal variations. Environ. Pollut. 227, 334–347.

Srivastava, N., Hinton, G., Krizhevsky, A., et al., 2014. Dropout: a simple way to prevent neural networks from overfitting. J. Mach. Learn. Res. 15 (1), 1929–1958.

Stowell, J.D., Geng, G., Saikawa, E., et al., 2019. Associations of wildfire smoke PM2. 5 exposure with cardiorespiratory events in Colorado 2011–2014. Environ. Int. 133, 105151.

Sun, Y., Zeng, Q., Geng, B., et al., 2019. Deep learning architecture for estimating hourly ground-level PM 2.5 using satellite remote sensing. IEEE Geosci. Remote Sens. Lett. 16 (9), 1343–1347.

Tao, M., Chen, L., Wang, Z., et al., 2014. A study of urban pollution and haze clouds over northern China during the dusty season based on satellite and surface observations. Atmos. Environ. 82, 183–192.

Tong, W., Li, L., Zhou, X., et al., 2019. Deep learning PM2.5 concentrations with bidirectional LSTM RNN. Air Qual. Atmos. Health 12, 411–423.

Turner, M.C., Krewski, D., Pope, C.A., et al., 2011. Long-term ambient fine particulate matter air pollution and lung cancer in a large cohort of never-smokers. Am. J. Respir. Crit. Care Med. 184, 1374–1381.

Venter, Z.S., Aunan, K., Chowdhury, S., et al., 2020. COVID-19 lockdowns cause global air pollution declines. Proc. Natl. Acad. Sci. 117(32), 18984–18990.

Wang, Y., Liu, C., Wang, Q., et al., 2021. Impacts of natural and socioeconomic factors on PM2. 5 from 2014 to 2017. J. Environ. Manage. 284, 112071.

Wang, W., Liu, X., Bi, J., et al., 2022. A machine learning model to estimate ground-level ozone concentrations in California using TROPOMI data and high-resolution meteorology. Environ. Int. 158, 106917.

Wang, X., Sun, W., 2019. Meteorological parameters and gaseous pollutant concentrations as predictors of daily continuous PM2.5 concentrations using deep neural network in Beijing–Tianjin–Hebei, China. Atmos. Environ. 211, 128–137.

Wei, P., Xie, S., Huang, L., et al., 2023. Spatial interpolation of regional PM2. 5 concentrations in China during COVID-19 incorporating multivariate data. Atmosp. Pollut. Res. 14 (3), 101688.

Xiao, Q., Geng, G., Liang, F., et al., 2020. Changes in spatial patterns of PM2. 5 pollution in China 2000–2018: impact of clean air policies. Environ. Int. 141, 105776.

Xu, X., Tong, T., Zhang, W., et al., 2020. Fine-grained prediction of PM2.5 concentration based on multisource data and deep learning. Atmos. Pollut. Res. 11, 1728–1737.

Xu, W., Wooster, M.J., Kaneko, T., et al., 2017. Major advances in geostationary fire radiative power (FRP) retrieval over Asia and Australia stemming from use of Himarawi-8 AHI. Remote Sens. Environ. 193, 138–149.

Xue, W., Zhang, J., Zhong, C., et al. Satellite-derived spatiotemporal PM2.5 concentrations and variations from 2006 to 2017 in China. Sci. Total Environ. 2020, 712, 134577.

Xue, Y., Li, Y., Guang, J., et al., 2020. Hourly PM2.5 estimation over Central and Eastern China Based on Himawari-8 Data. Remote Sens. 12, 855.

Xue, T., Zheng, Y., Tong, D., et al., 2019. Spatiotemporal continuous estimates of PM2.5 concentrations in China, 2000–2016: a machine learning method with inputs from satellites, chemical transport model, and ground observations. Environ. Int. 123, 345–357.

Yan, X., Zang, Z., Luo, N., et al., 2020. New interpretable deep learning model to monitor real-time PM2.5 concentrations from satellite data. Environ. Int. 144, 106060.

Yan, X., Zang, Z., Jiang, Y., et al., 2021. A Spatial-Temporal Interpretable Deep Learning Model for improving interpretability and predictive accuracy of satellite-based PM2.5. Environ. Pollut. 273, 116459.

Yao, L., Yang, L., Yuan, Q., Yan, C., et al., 2016. Sources apportionment of PM2. 5 in a background site in the North China Plain. Sci. Total Environ. 541, 590–598.

Yuchi, W., Brauer, M., Czekajlo, A., et al., 2022. Neighborhood environmental exposures and incidence of attention deficit/hyperactivity disorder: a population-based cohort study. Environ. Int. 161, 107120.

Zamani, J., Cao, M., Ni, C., et al., 2019. PM2.5 Prediction based on random forest, XGBoost, and deep learning using multisource remote sensing data. Atmosphere 10, 373.

Zhang, L., Wilson, J.P., MacDonald, B., et al., 2020. The changing PM2. 5 dynamics of global megacities based on long-term remotely sensed observations. Environ. Int. 142, 105862.

Zhang, C., Zhang, Y., Liu, X., et al., 2023. Characteristics and source apportionment of PM2. 5 under the dual influence of the Spring Festival and the COVID-19 pandemic in Yuncheng city. J. Environ. Sci. 125, 553–567.

Zoran, M.A., Savastru, R.S., Savastru, D.M., et al., 2020. Assessing the relationship between surface levels of PM2. 5 and PM10 particulate matter impact on COVID-19 in Milan, Italy. Sci. Total Environ. 738, 139825.

Further reading

Zhao, C., Pan, J., Zhang, L., 2021. Spatio-temporal patterns of global population exposure risk of PM2.5 from 2000–2016. Sustainability 13, 7427.